Journal of Pathology
J Pathol 2000; **192**: 221–228.
DOI: 10.1002/1096-9896(2000)9999:9999<::AID-PATH679>3.0.CO;2-B

Original Paper

Clonal patterns in phaeochromocytomas and MEN-2A adrenal medullary hyperplasias: histological and kinetic correlates†

Salvador J. Diaz-Cano[1,2]*, Manuel de Miguel[3], Alfredo Blanes[4], Robert Tashjian[2], Hugo Galera[3] and Hubert J. Wolfe[2]

[1] *Department of Pathology, St Bartholomew's and the Royal London School of Medicine and Dentistry, London, UK*
[2] *Department of Pathology, Tufts University – New England Medical Center, Boston, MA, USA*
[3] *Department of Pathology, University Hospital of Seville, Spain*
[4] *Department of Pathology, University Hospital of Málaga, Spain*

Correspondence to: Salvador J. Diaz-Cano, Department of Histopathology and Morbid Anatomy, The Royal London Hospital, Whitechapel, London E1 1BB, UK. E-mail: s.j.diaz-cano@mds.qmw.ac.uk

Received: 3 September 1999
Revised: 7 December 1999
Accepted: 24 March 2000
Published online: 26 June 2000

Abstract

The relationship among histological features, cell kinetics, and clonality has not been studied in adrenal medullary hyperplasias (AMHs) and phaeochromocytomas (PCCs). Thirty-four PCCs (23 sporadic and 11 MEN-2A (multiple endocrine neoplasia type 2A)-related tumours, the latter associated with AMH) from females were included in this study. Representative samples were histologically evaluated and microdissected to extract DNA and evaluate the methylation pattern of the androgen receptor alleles. At least two tissue samples (from the peripheral and internal zones in each tumour) were analysed with appropriate tissue controls run in every case. The same areas were selected for MIB-1 staining and *in situ* end labelling (ISEL). Malignant PCCs were defined by histologically confirmed distant metastases. All monoclonal AMH nodules from the same patient showed the same X-chromosome inactivated. Six sporadic PCCs revealed liver metastases (malignant PCC) and eight additional sporadic PCCs showed periadrenal infiltration (locally invasive PCC). All informative PCCs were monoclonal, except for five locally invasive PCCs and one benign PCC that revealed polyclonal patterns. Those cases also showed a fibroblastic stromal reaction with prominent blood vessels, focal smooth muscle differentiation, and significantly higher MIB-1 (126.8 ± 29.9) and ISEL (50.9 ± 12.8) indices. Concordant X-chromosome inactivation in nodules from a given patient suggests that MEN-2A AMH is a multifocal monoclonal condition. A subgroup of PCCs characterized by balanced methylation of androgen receptor alleles, high cellular turnover, and stromal proliferation also shows locally invasive features.

Keywords: phaeochromocytomas; adrenal medullary hyperplasias; MEN-2A; X-chromosome inactivation; proliferation; apoptosis; stromal reaction

Introduction

Phaeochromocytomas (PCCs), either sporadic or associated with multiple endocrine neoplasia type 2 (MEN-2), are arbitrarily distinguished from adrenal medullary hyperplasias (AMHs) [1,2], especially for large nodules in a multinodular background [3]; some reports have proposed nodule size (>1 cm) as the differentiating criterion [2,4]. Our knowledge of AMH comes from inherited conditions, especially MEN-2, where morphometry has been shown to be useful in distinguishing AMH from normal adrenal medulla [3].

The current diagnosis of malignant PCC requires the demonstration of metastases, defined by tumour growths in sites where chromaffin tissue is not present, such as lymph nodes, liver, and bone [2]. Locally invasive PCCs are characterized by variable invasion of periadrenal tissue and no evidence of distant metastases [5–7], but the association of local invasion with lymph node metastases and long-term outcome remain unknown [2]. Neoplasms are defined as clonal proliferations, in contrast to the heterogeneous composition of most normal tissues [8,9]; hence a monoclonal cell population which has arisen from heterogeneous normal tissues strongly suggests a neoplastic nature [7,10]. Different and variable success has been reported for several markers, but clonality still remains the hallmark of neoplasia. Clonal selection should also be the expression of kinetic advantage (high proliferation or abnormally low apoptosis) [7,10–12] resulting in dominant growths [7,8]. The relationship of clonality, cell kinetics (proliferation and apoptosis), and histological features has not been studied in AMH and PCC.

This study investigates the clonal pattern of sporadic and MEN-2A-associated AMH and PCC, based on the analysis of the methylation pattern of androgen receptor alleles (ARAs) using microdissected samples,

†Presented in part as abstracts at the Annual Meetings of the United States and Canadian Academy of Pathology in Washington, DC, 1996 and Orlando, FL, 1997.

and its correlation with kinetic and histological features.

Materials and methods

Case selection

Thirty-four PCCs from females (23 sporadic and 11 MEN-2A-related) were studied. Six sporadic PCCs were malignant (histologically confirmed liver metastases and elevated post-operative levels of catecholamines) and eight sporadic PCCs were locally invasive (periadrenal infiltration). The post-operative catecholamine levels were normal in both locally invasive and benign PCCs. Familial PCCs were associated with AMH, selected from 177 members (five generations) of known MEN-2A kindred and classified as benign. These patients were screened for C-cell hyperplasia – medullary thyroid carcinoma and demonstrated to carry a germline point mutation on codon 634 of the *RET* proto-oncogene by PCR-restriction fragment length polymorphism and sequencing [13]. AMH was defined according to standard criteria (expansion of the medullary compartment into areas of the gland where it is not normally present) [3], considering nodules larger than 1 cm as PCC [2,4].

All surgical specimens were serially sectioned, sampled according to standard protocols (1 block/cm of tumour-nodule), and had appropriate archival material available. The same areas in consecutive sections were used for each study and their cellular composition was confirmed in adjacent haematoxylin and eosin-stained sections.

Clonality analysis

DNA was extracted from two 20-μm unstained paraffin sections that included at least 100 cells per sample (about 0.4 mm^2), using a modified phenol–chloroform protocol [14]. Microdissected samples were systematically taken from the peripheral and internal zones of every tumour. The small size of most nodules precluded reliable topographic sampling; one sample was taken from the peripheral area of each nodule. Appropriate controls were included for each test (adrenal medulla, adrenal cortex, and periadrenal soft tissue). Only well-defined nodules from patients with a polyclonal pattern in the intervening adrenal medulla were included, to guarantee appropriate controls.

Half of each sample underwent Hha-I digestion (0.8 unit/μl; New England Biolabs, Beverly, MA, USA) and the other half was used as an undigested control. Both samples were equally processed, but excluding Hha-I in the undigested ones [10,15–17]. A mimicker (0.3 μg of double-stranded and Xho I-linearized ϕX174-RII phage) (Gibco-BRL, Gaithersburg, MD, USA) was included to test digestion completion after gel electrophoresis; incompletely digested samples were repurified and redigested with a higher Hha-I concentration. Hha-I was inactivated by phenol–chloroform extraction [14] and DNA was precipitated with ice-cold absolute ethanol in the presence of 0.3 M sodium acetate, pH 5.2 and resuspended in 10 μl of 10 mM Tris–HCl (pH 8.4), 50 mM KCl, 1.5 mM $MgCl_2$, and 100 μg/ml BSA. The first exon CAG repeat of the androgen receptor gene was amplified, according to the conditions shown in Table 1, in a Perkin-Elmer thermal cycler model 480 (Perkin-Elmer, Norwalk, CT, USA), using both digested and undigested DNA templates [16,17].

The whole PCR volume (10 μl) was electrophoresed into 8% non-denaturing polyacrylamide gels (0.75 mm) and run at 5 V/cm until the xylene cyanol band was within the bottom gel inch. The gels were fixed with 7% acetic acid (5 min), dried *in vacuo* (40 min, 80°C), and put inside a developing cassette containing one intensifying screen and preflashed films (Kodak XAR) facing the intensifying screen (16–48 h, −70°C). The autoradiograms were developed using a Kodak-Omat 100 automated processor (Kodak Co., Rochester, NY, USA).

Interpretation and inclusion criteria were as previously reported [10,18]. Only informative cases (two different alleles in undigested and digested controls) were included in the final analysis [10,16,17]. Allelic imbalance was densitometrically evaluated (EC model 910 optical densitometer, EC Apparatus Corporation, St Petersburg, FL, USA), considering evidence of monoclonality allele ratios $\geqslant 4:1$ in the normalized digested lanes. Lanes were normalized in relation to the corresponding undigested sample and controls. Additional allele bands in the tumour/nodule samples were only recorded if not present in the corresponding control.

In situ end labelling (ISEL) of fragmented DNA

Extensive DNA fragmentation associated with apoptosis was detected by ISEL as previously reported [12,19]. Sections were routinely deparaffinized, hydrated, and incubated with 2× SSC buffer (80°C, 20 min). After pronase digestion (500 μg/ml, 25 min, room temperature), the sections were incubated with the Klenow fragment of *Escherichia coli* DNA polymerase I under appropriate conditions (20 units/ml, 100 μM of each dNTP with a proportion of 11-digoxigenin-dUTP/dTTP of 0.35/0.65, 2 h at 37°C). The digoxigenin-labelled DNA fragments were detected using anti-digoxigenin polyclonal antibody labelled with alkaline phosphatase (1/100 dilution; Boehringer-Mannheim, Germany). The reaction was developed with nitroblue-tetrazolium and X-phosphate under microscopic control [12], and the sections were counterstained with diluted haematoxylin (25%). Appropriate controls were run, including positive (reactive lymph node), negative (omitting DNA polymerase I), and enzymatic (DNase I digestion before end labelling). The enzymatic controls allowed a reliable positivity threshold to be established in each sample.

Table 1. Primer sequences and PCR cycling conditions for the amplification of polymorphic DNA regions

Primers	Primer sequences	Tandem repeat/PCR product
AR-a	5′- CCG AGG AGC TTT CCA GAA TC -3′	CAG repeat/215–300 bp
AR-b	5′ TAC GAT GGG CTT GGG GAG AA -3′	

All reactions were run with 1.5 mM of $MgCl_2$, using 0.3 μM of each primer and 200 μM of each dNTP (including 7-deaza-dGTP instead of dGTP) in the HUMARA amplification. The PCR products were internally labelled with 0.3 μCi of α[^{32}P]-dTTP (800 Ci/mmol, 10 mCi/ml; New England Nucleotide, Boston, MA, USA). All reactions were run in duplicate using 1 μl of template.
A long denaturation (4 min) and extension (90 s) were used in the first three cycles for each set of primers and a 'hot start' was included. The annealing temperature was 55°C and the number of cycles was experimentally optimized to 28.

Immunohistochemical expression of MIB-1, S-100 protein, smooth muscle actin, and desmin

The sections were mounted on positively charged microscope slides (Superfrost Plus, Fisher Scientific, NJ, USA), baked at 60°C for 2 h, and routinely dewaxed and rehydrated. The endogenous peroxidase activity was quenched (0.5% H_2O_2 in methanol, 10 min) and the antigens were retrieved (20 min in 10 mM citrate buffer, pH 6.0, using microwave treatment at 600 W). After treatment with polyclonal horse serum (20 min, 1/100 dilution) (Dako, Denmark), the sections were incubated with monoclonal primary antibodies (overnight, 4°C) at 1 μg/ml for MIB-1 (Oncogene Science, Cambridge, MA, USA), S-100 protein, smooth muscle antin, and desmin (Dako, Denmark). The reaction was developed using biotinylated anti-mouse antibody (30 min, 1/200 dilution) (Dako, Denmark), peroxidase-labelled avidin–biotin complex (60 min, 1/100 dilution) (Dako, Denmark), and 3,3′-diaminobenzidine tetrahydrochloride with 0.3% H_2O_2 as chromogen (Sigma Co., St. Louis, MO, USA). The sections were counterstained with haematoxylin. Both positive and negative (omitting the primary antibody) controls were simultaneously run.

Quantification of positive nuclei

At least 50 high power fields (HPF), or the complete lesion if smaller (50 HPF = 7.6 mm^2), were screened in each pathological group, beginning in the most cellular area. Both the number of positive nuclei per HPF and the number of proliferating cells intercepted by the microscope field diameter were registered. The last score and the formula $N=(n\pi/4)^2$ (N is the number of estimated cells per HPF and n is the number of cells intercepted by the microscope field diameter) [20,21] were used to estimate the number of proliferating cells per HPF. Both the average and the standard deviation (SD) were calculated in each patient and pathological condition and expressed per 1000 proliferating cells. Only nuclei with staining features similar to those of their corresponding positive control were counted for a given parameter (MIB-1, ISEL).

Statistical analysis

The average and SD of every quantitative variable were compared in each pathological condition (adrenal medullary hyperplasia, benign PCC, locally invasive PCC, and malignant PCC) and per tumour/nodule compartment by two-tailed Student's t-test or analysis of variance (ANOVA) for non-parametric distribution, and considered statistically significant if $p<0.05$.

Results

We found 34 AMH nodules in 11 MEN-2A patients (three patients contributing two nodules, four cases with three nodules, and four adrenals with four nodules). Four nodules from two patients (two nodules each) were considered non-informative and excluded from further analysis. Twenty-seven nodules revealed the same X-chromosome inactivated in nodules from the same patient (Figure 1). The remaining three nodules (from two patients) showed a polyclonal pattern. As no reliable differences accurately distinguished true polyclonal lesions from clonal proliferations of two divergent cell populations, these cases were also excluded.

Concordant methylation patterns of ARAs were found in nine informative patients: one contributing two nodules, four providing three nodules, and four giving four nodules. Cells from informative patients inactivate either the smaller or the larger allele, resulting in a 50% probability of finding the same allele methylated in cell-to-cell comparison. Assuming an equal and independent probability of ARA methylation at the cellular level, each tissue from an informative female can be revealed to be polyclonal, monoclonal with preferential methylation of the larger allele, or monoclonal with the smaller allele predominating [22]. Equal *a priori* probability for each pattern should be expected ($p=1/3$) and tissue ARA patterns from informative patients would be concordant with a probability of $2(1/3)^n$, where 2 is the number of alleles and n is the number of lesions compared. Therefore, identical methylation patterns of ARAs in these nine patients would be randomly found with a probability of $2\ ((1/3)^2)^1\ ((1/3)^3)^4\ ((1/3)^4)^4 = 2\ (1/3)^2\ (1/3)^{12}\ (1/3)^{16} = 2\ (1/3)^{30} = 9.71\times10^{-15}$.

Concordant methylation patterns of ARAs were observed in peripheral and internal samples of each PCC. Of 29 informative patients with PCC, 23 PCCs revealed a monoclonal pattern (17 benign, including eight sporadic and nine in MEN-2A patients, and six malignant) and six sporadic PCCs (five locally invasive

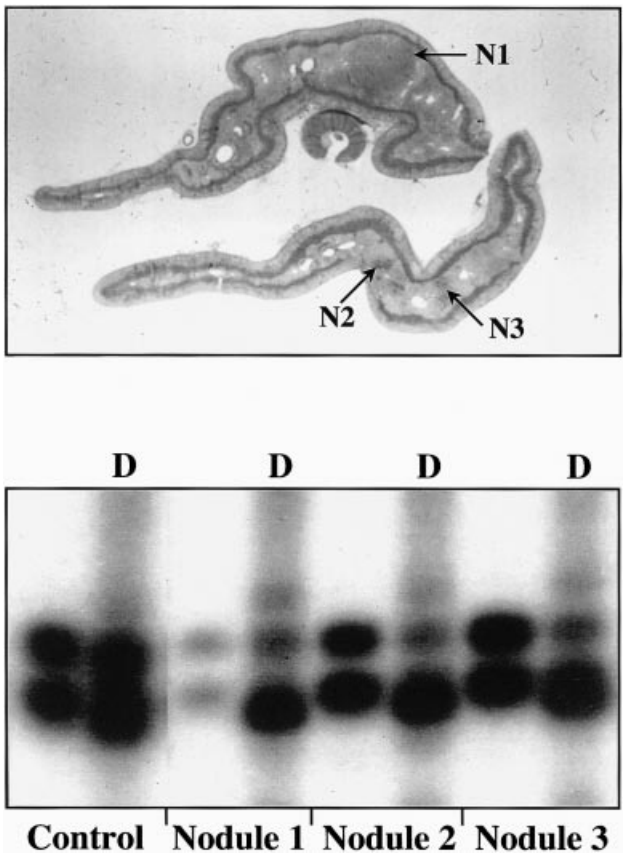

Figure 1. Clonality in adrenal medullary hyperplasias. The same X-chromosome was inactivated in monoclonal nodules from a given patient. The densitometric analysis revealed an allele ratio greater than 4/1, low/high in this case. The histology shows the nodules dissected, while the intervening adrenal medulla was used as a control. D = digested sample

and one benign) showed a polyclonal pattern (Figure 2). Histology revealed a distinctive stromal reaction in three AMH nodules and six PCCs (all polyclonal), comprising prominent spindle cell proliferation with focal cytoplasmic expression of smooth muscle actin and desmin and prominent blood vessels (Figure 3). Stromal contamination was excluded by repeated careful microdissections that confirmed the same polyclonal pattern. No differences were detected whether or not the samples were boiled during extraction.

A progressive increase in both MIB-1 and ISEL indices was revealed in the sequence AMH – benign PCC – malignant PCC, but with no statistically significant differences (Table 2). The only significant differences were observed in locally invasive PCC, which showed the highest indices ($p < 0.001$) (Table 2 and Figures 3 and 4). No topographic differences were detected for any marker or pathological condition (Table 2).

Discussion

Different conclusions emerged for AMH and PCC. AMH nodules in MEN-2A have been proven to be mainly monoclonal and have revealed the same X-chromosome inactivated in a given patient; this suggests that clonal expansions target precursors before they spread in the adrenal medulla and that nodular AMH is a clonal and multifocal lesion. In sporadic PCC, a distinctive histological and kinetic profile correlates with a polyclonal pattern and periadrenal infiltration.

Monoclonal AMH nodules (27/30 informative nodules, 90.0%) showed the same ARA preferentially methylated in a given patient, suggesting that a common progenitor contributed to such lesions and supporting multifocal rather than multicentric growth, as proposed for other lesions [23–25]. The internodular adrenal medulla had to be polyclonal to consider the case informative, thus precluding any conclusion for diffuse AMH. The presence of monoclonal AMH nodules which have developed in polyclonal diffuse AMH supports their neoplastic nature [8,9] and a multistep tumourigenesis in the adrenal medulla of MEN-2A patients [3,4,26]. Their concordant monoclonal pattern in a given patient supports early clonal expansion of precursor cells between the random X-chromosome inactivation and their spreading in the adrenal medullary anlage [7,10], resulting in PCC when other genes are targeted and genetic alterations accumulate. Supportive evidence showed at least one microsatellite abnormality of tumour suppressor genes in 75% of MEN-2A PCCs (manuscript submitted) and the same X-chromosome preferentially inactivated in both thyroid lobes in monoclonal C-cell hyperplasias from 8/9 informative patients from these kindreds (89%) (manuscript submitted). However, two other reasons for monoclonal patterns must be excluded. Firstly, contiguous cellular regions of the same lineage ('patch size' concept) and embryological factors determine the clonal pattern in polymorphic tissues. Any kinetic advantage of cell groups sharing the same inactivated X-chromosome would determine their preferential growth and mosaic patch size (non-random skewness of X-chromosome inactivation) in the early stages [7,8,10,11]. Our controls and sampling technique ($\geqslant 100$ cells) exclude non-random skewness or patch size variability as causes [7,10]. In addition, patch size mosaicism could not explain AMH nodules with concordant X-chromosome inactivation. Secondly, PCR bias against the larger ARA could contribute to preferential amplification of the smaller ARA. Our DNA extraction protocol [14,27] included a long protein digestion and demonstrated an average DNA size of about 1 kb (data not shown), excluding DNA degradation as the cause. Our PCR design [10,17,28,29] also included long denaturation – extension in the first three cycles and 7-deaza-dGTP in the amplification mixture to exclude PCR bias (Table 1), as confirmed in the cases showing the larger ARA methylated (Figure 2).

The first clonality study in MEN-2A PCC reported only one glucose-6-phosphate dehydrogenase isoenzyme in tumour tissue from patients heterozygous for

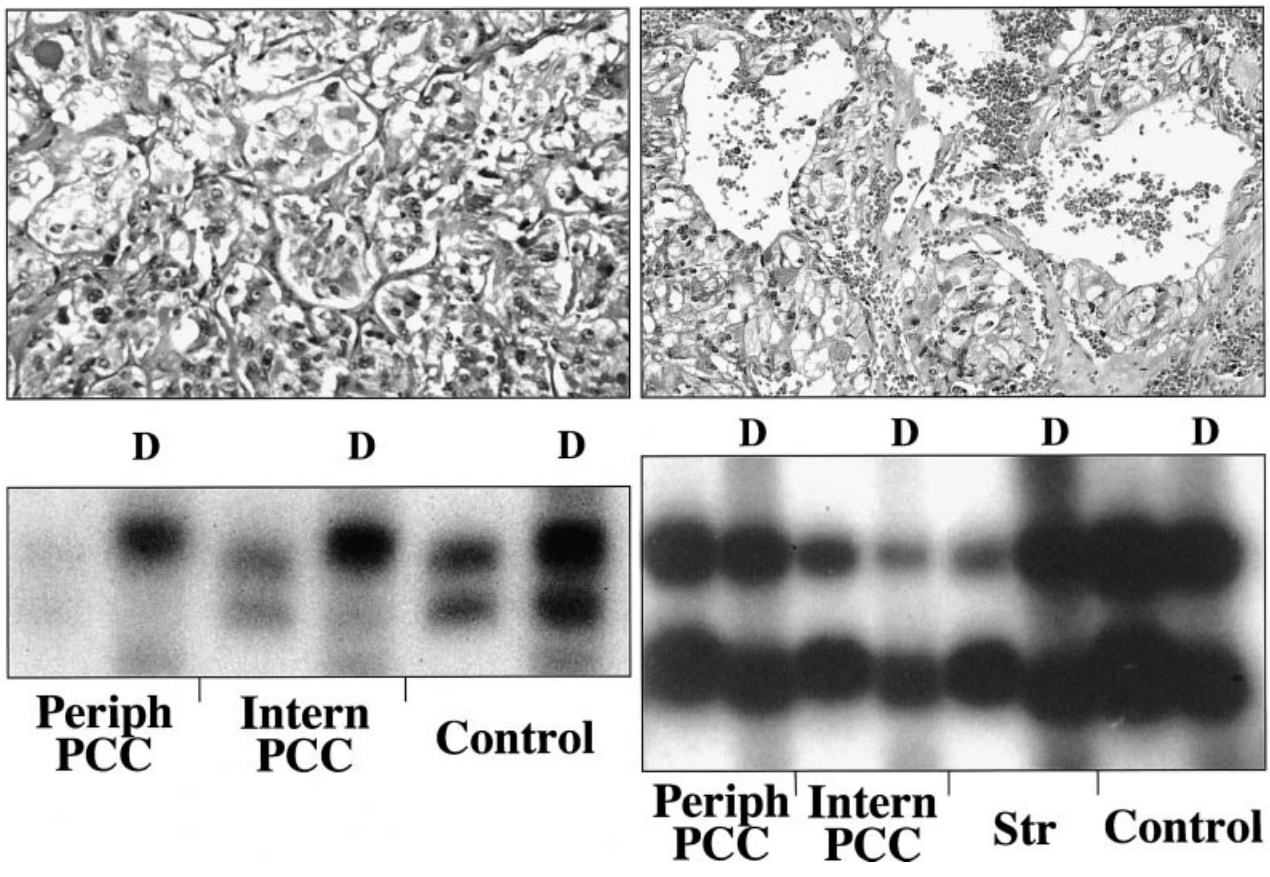

Figure 2. Histology and clonality in phaeochromocytomas (PCCs). Concordant methylation patterns of androgen receptor alleles were found in peripheral and internal samples from the same tumour. Polyclonal cases (right-hand side of the panel) revealed stromal proliferation with balanced methylation of androgen receptor alleles (Haematoxylin and eosin, $\times 300$ left and $\times 150$ right). D = digested sample

that marker [30,31]. The authors suggested initial mutations producing multiple clones of defective cells as a preneoplastic condition, which would progressively evolve into monoclonal growths by clone selection [30,31]. Although the histopathological features have not been characterized, the initial stage in our study would be the polyclonal diffuse AMH that results in monoclonal nodular AMH by early clonal expansions. The migration of neural crest cells into the adrenal medulla proceeds in finger-like projections around the blood vessel that penetrate the cortex from the caudal aspect [32] and help to explain the multinodular pattern if early clonal expansion affects the precursor cells. Our results also question the diagnostic utility of nodule size to distinguish AMH from PCC [2]. No reliable histological criterion distinguishes large nodules in a multinodular AMH from small PCC, and morphometry only distinguishes AMH from normal adrenal medulla [3]. Tumour-nodule size is a time-dependent parameter that revealed a monoclonal pattern even in small nodules, an unsurprising finding in processes with early neoplastic transformation, such as most inherited tumour syndromes [33,34], including MEN-2.

Monoclonal PCC (23/29, 79.3%) revealed the same X-chromosome inactivated in the peripheral and internal compartments. All MEN-2A PCCs revealed this feature and multinodular AMH, in agreement with the high prevalence of monoclonal patterns found in these AMH nodules (27/30, 90%). A polyclonal pattern was revealed in sporadic locally invasive PCCs (6/29, 21.7%), which could be explained under the three following circumstances. Firstly, X-chromosome inactivation was tested using methylation-sensitive restriction endonucleases. Both incomplete endonuclease digestion [7] and aberrant hypermethylation (due to tumour progression or abnormal imprinting) [10] would result in false polyclonal patterns in monoclonal tissues. The completion of endonuclease digestion was tested using a viral mimicker and both the long denaturation (16 h) and the activity of Hha-I on single-stranded DNA would ensure complete digestion of the denatured DNA related to embedding and extraction. Repeated polyclonal patterns were obtained using non-boiled templates. We are currently testing methylation in these tumours. Secondly, any significant contamination with normal cells could be excluded by a consistent polyclonal pattern after careful and repeated microdissection. Contamination with normal cells would determine a polyclonal gel pattern in monoclonal tissues [7,10]. Other systems such as laser-capture microdissection can decrease contamination, but the results reported for samples of around 100 cells are identical using manual or laser-capture microdis-

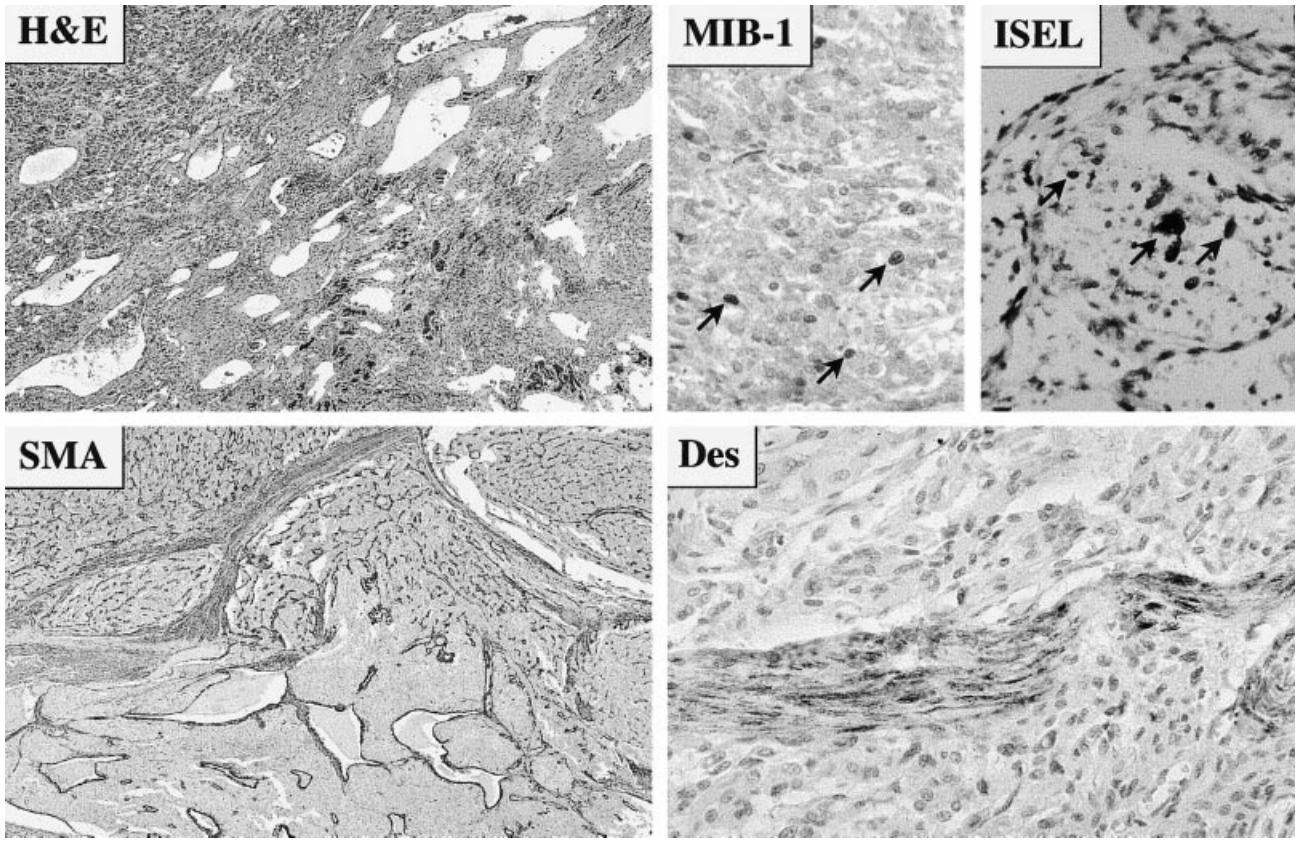

Figure 3. Locally invasive phaeochromocytomas. These neoplasms revealed numerous dilated blood vessels associated with stromal reaction (haematoxylin and eosin, ×80). They also showed a high cellular turnover with significantly higher MIB-1 (avidin–biotin complex, ×160) and *in situ* end labelling (alkaline phosphatase, ×160) indices than benign and malignant PCCs (arrows point to positive nuclei). Extensive expression of smooth muscle actin (avidin–biotin complex, ×80) was found in the stromal component, with only focal presence of desmin-positive cells (avidin–biotin complex, ×160)

section [35]. In the present series, the stromal reaction was revealed as polyclonal and excluded in careful microdissections, but PCC still showed a polyclonal pattern. These non-epithelial components have been proposed as a key element of epithelial growth by either secretion of stimulatory factors or lack of an inhibitory factor [36]. Thirdly, clonal proliferation of cells showing different X-chromosomes inactivated (as expression of an unfinished process of cell selection) also results in polyclonal patterns, but requires additional markers such as loss of heterozygosity of tumour suppressor genes [7] to prove it (manuscript in preparation). These polyclonal patterns would represent true polyclonal proliferations only if precursor clonal expansions occurred after the random X-chromosome inactivation [7,10].

The second remarkable aspect of PCC with a polyclonal pattern was the high cellular turnover demonstrated by high MIB-1 and ISEL indices. We have observed endocrine tumours with regressive changes (stromal proliferation, prominent blood vessels, and increased apoptosis index) (Figure 5) [11,29], but with a positive proliferation–apoptosis ratio and slow tumour growth. They also showed variable periadrenal invasion and stromal overgrowth with smooth muscle differentiation, but no evidence of distant metastases. Stromal and vascular proliferations in tumours have been described as a reaction to

Table 2. Quantification of nuclear MIB-1 expression and in situ end labeling in adrenal medullary hyperplasias and pheochromocytomas by topographic compartment

		MIB-1 index		ISEL index	
		Peripheral	Internal	Peripheral	Internal
MEN-2A	AMH	15.3±3.9	16.7±3.6	2.1±0.3	3.0±0.4
	PCC	28.3±4.3	31.1±5.6	8.3±1.0	9.7±1.3
Sporadic PCC	Benign	30.2±4.4	33.7±5.3	7.4±1.3	7.1±1.6
	Locally invasive	126.8±29.9	132.5±33.2	50.9±12.8	46.8±15.1
	Malignant	70.1±20.6	74.0±19.9	22.3±5.7	25.4±6.8

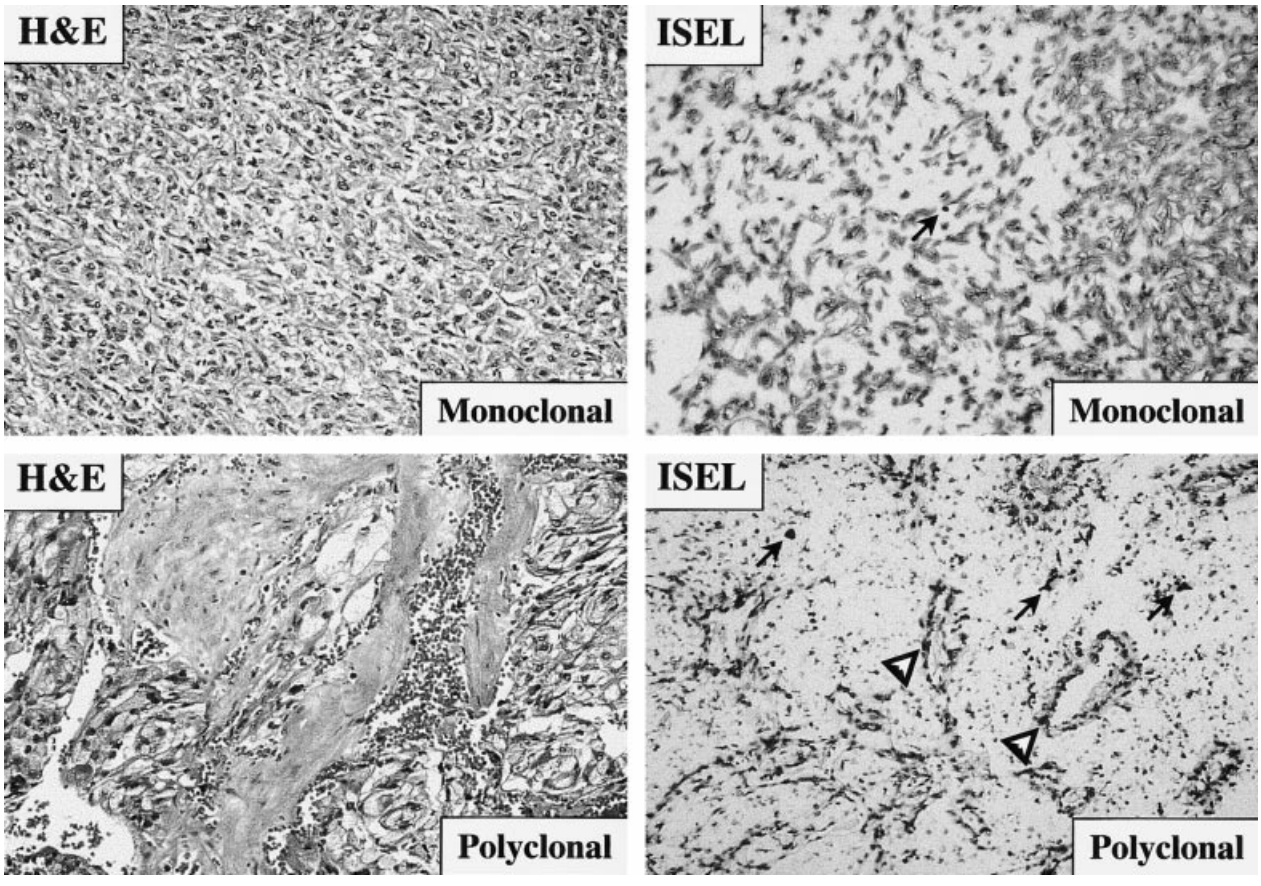

Figure 4. Histological features and apoptosis in adrenal medullary hyperplasias. Polyclonal nodules showed hyalinized stroma with dilated blood vessels and a high *in situ* end labelling index. Arrows point to positive nuclei and arrow-heads to the positive labelling of endothelial cells. (All figures $\times 80$; ISEL developed with alkaline phosphatase)

invasion or as an expression of regression. Interstitial fibrin deposition from leaky tumour vessels provides a provisional stroma that serves to regulate the influx of inflammatory cells and facilitates the inward migration of new blood vessels and fibroblasts, the mature tumour stroma [37]. That process has demonstrated a pivotal role in promoting tumour growth [38]. Those features present in locally invasive PCC would explain the high proliferation rates and the presence of tetraploid cells [39] secondary to non-disjunctional mitoses. This cellular process would end in lethal genetic changes and an increased apoptotic rate (Figure 5). We can speculate that the expansive process would contribute to the periadrenal invasion in a non-metastasizing neoplasm, but it needs additional studies, especially focused on tumour cell adhesion and its association with lymph node metastases and patient outcome.

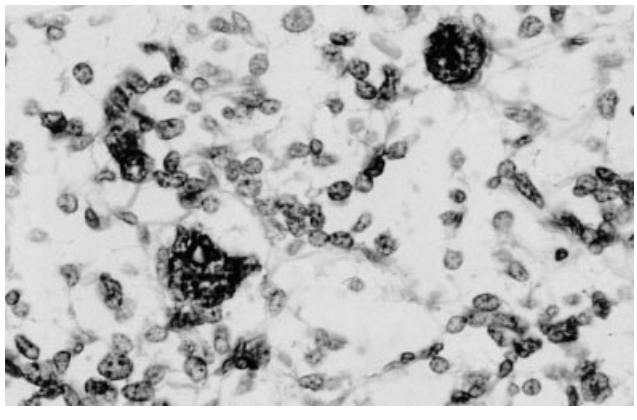

Figure 5. Nuclear atypia and apoptosis in phaeochromocytomas. Tumours with regressive changes and a stromal reaction revealed atypical nuclei with positive *in situ* end labelling (alkaline phosphatase, $\times 220$)

In conclusion, nodular AMH is essentially a multifocal monoclonal proliferation that shows the same X-chromosome inactivated in AMH nodules from a given patient, suggesting an early clonal expansion of adrenal medullary precursors. A subgroup of PCCs with a polyclonal pattern, high cellular turnover, and stromal proliferation also shows locally invasive features. This group needs additional studies to define its biological meaning.

References

1. Neumann HP, Berger DP, Sigmund G, *et al*. Pheochromocytomas, multiple endocrine neoplasia type 2, and von Hippel–Lindau disease. *N Engl J Med* 1993; **329**: 1531–1538.
2. Lack EE. *Tumors of the Adrenal Gland and Extra-adrenal Paraganglia*. Armed Forces Institute of Pathology: Washington, DC, 1997.
3. DeLellis RA, Wolfe HJ, Gagel RF, *et al*. Adrenal medullary

hyperplasia. A morphometric analysis in patients with familial medullary thyroid carcinoma. *Am J Pathol* 1976; **83**: 177–196.
4. Carney JA, Sizemore GW, Sheps SG. Adrenal medullary disease in multiple endocrine neoplasia, type 1. Pheochromocytoma and its precursors. *Am J Clin Pathol* 1976; **66**: 279–290.
5. Diaz-Cano SJ, de Miguel M, Galera-Davidson H, Wolfe HJ. Are locally invasive pheochromocytomas biologically distinct from benign chromaffin neoplasms? *Pathol Int* 1996; **46** (Suppl 1): 223a (Abstract).
6. Díaz-Cano SJ, Tashjian R, de Miguel M, *et al*. Distinctive clonal and histological patterns in locally invasive pheochromocytomas. *Lab Invest* 1997; **76**: 153A (Abstract).
7. Diaz-Cano SJ. Clonality studies in the analysis of the adrenal medullary proliferations: application principles and limitations. *Endocr Pathol* 1998; **9**: 301–316.
8. Nowell PC. The clonal evolution of tumor cell populations. *Science* 1976; **194**: 23–28.
9. Fialkow PJ. Clonal origin of human tumors. *Biochim Biophys Acta* 1976; **458**: 283–321.
10. Diaz-Cano SJ, Blanes A, Wolfe HJ. PCR-based techniques for clonality analysis of neoplastic progression. Bases for its appropriate application in paraffin-embedded tissues. *Diagn Mol Pathol (in press)*.
11. Salomon RN, Diaz-Cano S. Introduction to apoptosis. *Diagn Mol Pathol* 1995; **4**: 235–238.
12. Diaz-Cano SJ, Garcia-Moliner M, Carney W, Wolfe HJ. Bcl-2 expression and DNA fragmentation in breast carcinoma. Pathologic and steroid hormone receptors correlates. *Diagn Mol Pathol* 1997; **6**: 199–208.
13. Gagel RF, Cote GJ, Martins Bugalho MJ, *et al*. Clinical use of molecular information in the management of multiple endocrine neoplasia type 2A. *J Intern Med* 1995; **238**: 333–341.
14. Diaz-Cano SJ, Brady SP. DNA extraction from formalin-fixed paraffin-embedded tissues: protein digestion as a limiting step for retrieval of high quality DNA. *Diagn Mol Pathol* 1997; **6**: 342–346.
15. Allen RC, Zoghbi HY, Moseley AB, Rosenblatt HM, Belmont JW. Methylation of Hpa II and Hha I sites near to the polymorphic CAG repeat in the human AR gene correlates with X chromosome inactivation. *Am J Hum Genet* 1992; **51**: 1229–1239.
16. Mutter GL, Chaponot ML, Fletcher JA. A polymerase chain reaction assay for non-random X chromosome identifies monoclonal endometrial cancer and precancers. *Am J Pathol* 1995; **146**: 501–508.
17. Mutter GL, Boynton KA. PCR bias in amplification of AR alleles, a trinucleotide repeat marker used in clonality studies. *Nucleic Acids Res* 1995; **23**: 1411–1418.
18. Mutter GL, Boynton KA. X chromosome inactivation in the normal female genital tract: implications for identification of neoplasia. *Cancer Res* 1995; **55**: 5080–5084.
19. Wijsman JH, Jonker RR, Keijzer R, van de Velde CJH, Cornelisse CJ, van Dierendonck JH. A new method to detect apoptosis in paraffin sections: *in situ* end-labeling of fragmented DNA. *J Histochem Cytochem* 1993; **41**: 7–12.
20. Simpson JF, Dutt PL, Page DL. Expression of mitosis per thousand cells and cell density in breast carcinomas. A proposal. *Hum Pathol* 1992; **23**: 608–611.
21. Diaz-Cano SJ, Leon MM, de Miguel M, Galera-Davidson H, Wolfe HJ. Mitotic index quantification: different approaches and their value in adrenal cortical proliferative lesions. *Lab Invest* 1996; **74**: 170A (Abstract).
22. Diaz-Cano SJ, Wolfe HJ. Clonality in Kaposi's sarcoma [letter; comment]. *N Engl J Med* 1997; **337**: 571–572.
23. Sidransky D, Frost P, Von Eschenbach A, Oyasu R, Preisinger AC, Vogelstein B. Clonal origin of bladder cancer. *N Engl J Med* 1992; **326**: 737–740.
24. Rabkin CS, Janz S, Lash A, *et al*. Monoclonal origin of multicentric Kaposi's sarcoma lesions. *N Engl J Med* 1997; **336**: 988–993.
25. Quade BJ, McLachlin CM, Soto-Wright V, Zuckerman J, Mutter GL, Morton CC. Disseminated peritoneal leiomyomatosis. Clonality analysis by X chromosome inactivation and cytogenetics of a clinically benign smooth muscle proliferation. *Am J Pathol* 1997; **150**: 2153–2166.
26. Khosla S, Patel VM, Hay ID, *et al*. Loss of heterozygosity suggests multiple genetic alterations in pheochromocytomas and medullary thyroid carcinomas. *J Clin Invest* 1991; **87**: 1691–1699.
27. Brady SP, Magro CM, Diaz-Cano SJ, Wolfe HJ. Analysis of clonality of atypical cutaneous lymphoid infiltrates associated with drug therapy by PCR/DGGE. *Hum Pathol* 1999; **30**: 130–136.
28. Alman BA, Pajerski ME, Diaz-Cano S, Corboy K, Wolfe HJ. Aggressive fibromatosis (desmoid tumor) is a monoclonal disorder. *Diagn Mol Pathol* 1997; **6**: 98–101.
29. Diaz-Cano SJ, de Miguel M, Blanes A, Tashjian R, Galera H, Wolfe HJ. Clonality as expression of distinctive cell kinetic patterns in nodular hyperplasias and adenomas of the adrenal cortex. *Am J Pathol* 2000; **156**: 311–319.
30. Baylin SB, Gann DS, Hsu SH. Clonal origin of inherited medullary thyroid carcinoma and pheochromocytoma. *Science* 1976; **193**: 321–323.
31. Baylin SB, Hsu SH, Gann DS, Smallridge RC, Wells SA. Inherited medullary thyroid carcinoma: a final monoclonal mutation in one of multiple clones of susceptible cells. *Science* 1978; **199**: 429–431.
32. Crowder RE. The development of the adrenal gland in man with special reference to origin and ultimate location of cell types and evidence in favour of the 'cell migration' theory. *Carnegie Inst Contrib Embryol* 1957; **251**: 193–210.
33. Knudson AG Jr. Mutation and cancer: statistical study of retinoblastoma. *Proc Natl Acad Sci U S A* 1971; **68**: 820–823.
34. Knudson AG Jr, Hethcote HW, Brown BW. Mutation and childhood cancer: a probabilistic model for the incidence of retinoblastoma. *Proc Natl Acad Sci U S A* 1975; **72**: 5116–5120.
35. Sirivatanauksorn Y, Sirivatanauksorn V, Bhattacharya S, *et al*. Evolution of genetic abnormalities in hepatocellular carcinomas demonstrated by DNA fingerprinting. *J Pathol* 1999; **189**: 344–350.
36. Thomas GA, Williams D, Williams ED. The clonal origin of thyroid nodules and adenomas. *Am J Pathol* 1989; **134**: 141–147.
37. Nagy JA, Brown LF, Senger DR, *et al*. Pathogenesis of tumor stroma generation: a critical role for leaky blood vessels and fibrin deposition. *Biochim Biophys Acta* 1989; **948**: 305–326.
38. Dvorak HF, Sioussat TM, Brown LF, *et al*. Distribution of vascular permeability factor (vascular endothelial growth factor) in tumors: concentration in tumor blood vessels. *J Exp Med* 1991; **174**: 1275–1278.
39. Gonzalez-Campora R, Diaz Cano S, Lerma-Puertas E, *et al*. Paragangliomas. Static cytometric studies of nuclear DNA patterns. *Cancer* 1993; **71**: 820–824.